A Parallel FDTD Tool for the Solution of Large Dosimetric Problems: an Application to the Interaction between Humans and Radiobase Antennas

Luca Catarinucci[1], Paolo Palazzari[2], Luciano Tarricone[1]

[1] Dip. Ingegneria dell'Innovazione, University of Lecce, Via Monteroni, 73100, Lecce, Italy
[2] ENEA – HPCN Project - C.R. Casaccia -- S. Maria di Galeria, Rome, Italy

Abstract — **The rigorous theoretical solution of the human exposure to the near-field of radiobase antennas requires a heavy computational effort. In this paper we propose a full-wave solution based on the implementation of a Finite-Difference Time-Domain method on parallel computers, such as the APE-Quadrics SIMD machine with 512 processors. The cases of several GSM real antennas interacting with a numerical phantom proposed by the Visible Human Project are solved, demonstrating the amenability of the approach and its accuracy for a point-evaluation of all the relevant parameters (E and H fields, as well as SAR or local currents) with a millimeter-resolution.**

I. Introduction

The rapid diffusion of wireless technologies has focussed the attention on the potential risks for human health due to the exposure to electromagnetic (EM) fields. The problem, not new, is now a hot topic both for scientific research, and for its political and social implications.

Among the several EM sources, a particular interest has been addressed, till now, to cellular phones [1,2], whilst a much smaller emphasis has been reserved to radiobase station antennas (RBAs) [3]. Nonetheless, the exposure to the near-field (NF) of such devices is a relevant issue for a large class of workers, spending long daily time intervals in the proximity of RBAs (for instance, employees involved in radio-communication apparata installation and maintenance, or working over building roofs hosting RBAs).

The NF interaction between RBAs and humans is a difficult problem. It has been attacked with experimental approaches [4,5], using homogeneous or simplified human phantoms. A numerical solution, on the other hand, is potentially attractive, because of the several accurate numerical phantoms developed in the recent past, and the large variety of rigorous numerical EM techniques proposed in the literature. Unfortunately, a numerical accurate solution is quite hard, because of the huge computational effort required. In fact, in many cases, panel RBAs have a leading dimension D of nearly 2 meters, with consequent far-field distances which can easily reach 10-20 meters (using classical D^2/λ or $2D^2/\lambda$ relationships [6]). Therefore, the use of a full-wave solver, necessary for a rigorous NF analysis, is unaffordable with standard computational techniques. In such a framework, the development of a new computer tool, able to give a numerical rigorous solution to the RBA-human NF interaction problem, has several relevant goals, such as:

i) the evaluation of dosimetric parameters in a human subject exposed to a RBA and the consequent potential health risks

ii) the evaluation of the accuracy of experimental apparata, using for instance the homogeneous phantom approximation

iii) the evaluation of the accuracy of simplified approaches, using the far-field approximation [3].

In this paper, a fullwave numerical solution is proposed for the exposure of human beings to the NF of real RBAs used for the GSM mobile system. The solution here proposed is based on the implementation of a Finite-Difference Time-Domain (FDTD) approach on a parallel computer of the APE/Quadrics family. The Visible Human Project (VHP) numerical phantom is used.

The paper is structured as follows. In Section II the parallel FDTD approach is described, explaining the choice of the parallel computer platform, as well as the parallel algorithm. In Section III a short review is given on the used numerical phantom. In Section IV results are given, validating the proposed FDTD code, and estimating the human exposure to the NF of several real RBAs. Finally, conclusions are drawn.

II. Parallel FDTD on APE/Quadrics Platform

The FDTD approach is quite well-known and used for a large class of EM problems, due to its high versatility. A wide literature is available about FDTD, and this is not the appropriate context for a detailed description of the method. We just recall here that, among the several possible boundary conditions [7-9], Mur's absorbing boundary conditions (ABC) [7] are used. In fact, even though PML ABC [8-9] can be more accurate, they are more time-consuming, and their implementation on parallel architectures such as the ones here adopted is not trivial at all. Anyway, Mur's ABC guarantee an accuracy appropriate for the problem, as demonstrated in the following. Moreover, the classical relationships reported in [10,11] are used to guarantee spatial and time stability.

The elected architecture is the APE/Quadrics series [12]. It is a so-called Single-Instruction Multiple-Data (SIMD) platform. A SIMD platform is a multiprocessor architecture where every processor performs the same operation on different data in the mean time, and is quite amenable for an efficient parallel implementation of the FDTD scheme.

A. Parallel implementation

On a machine with n processors, the whole computation domain is divided into n sub-domains (with equal volume and shape); each sub-domain is assigned to a processor and adjacent sub-domains are assigned to adjacent processors (both the algorithm and the machine implementing it have 3D topology). The EM field components are contemporarily updated in each processor. When the computation updates a field component on the border of the domain, some values belonging to the border of the adjacent domain are required: in order to avoid communications during the computations, each sub-domain is surrounded by the border cells of the other domain. These border values are communicated after the updating phase.

The implementation of the proposed algorithm on the APE/Quadrics architecture guarantees very high speed-ups, as well as the possibility of managing large memory requirements. This is especially due to the small granularity of the FDTD integration scheme, rendering this problem very well suited to be implemented on massively parallel systems.

III. Numerical phantoms

A relevant role in the accurate solution of the addressed problem is played by the numerical technique utilized to represent the electromagnetic properties of the exposed human subject. The use of an appropriate numerical phantom, in fact, is the attractive issue to overcome the real problem of several proposed experimental techniques, using homogenous representations of the human body,

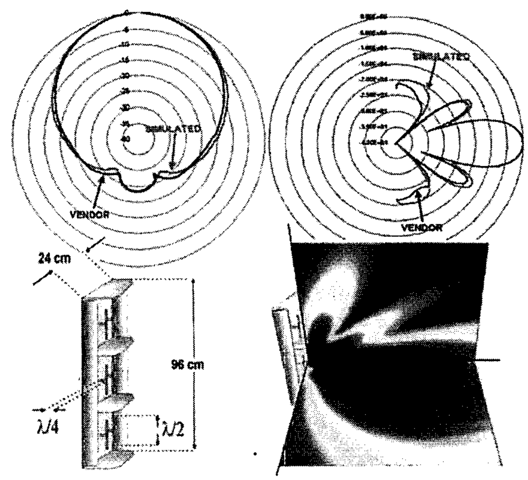

Fig. 1: H and E-plane radiation patterns for RBA K730685. The colour graph reports E-field levels (red for high-intensity areas, blue for low-level areas)

with a consequent approximation error sometimes not adequate to the goals of a radio-protection analysis.

The story of the development of accurate numerical phantoms is rich and long, and we address to the

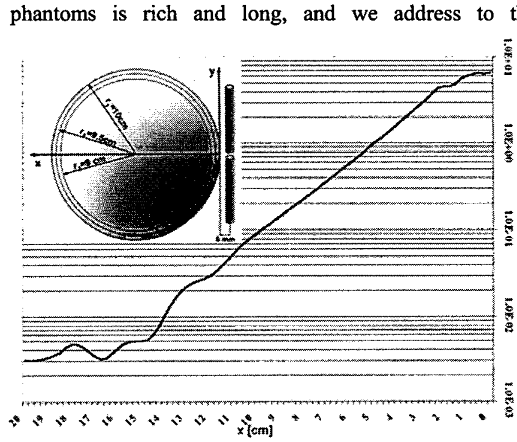

Fig. 2: The 10g-SAR behavior along x-axis. The input power is 1W.

specialized literature the interested reader [13-16]. In this work we refer to one of the most appreciated phantoms, the one proposed by the Visible Human Project (VHP) at Yale University. Yale phantom derives from the segmentation of the Trasmission Computerized (CT) x-Ray termography torso+head and MRI head slices of two living human males. The manually segmented 129 x-ray CT transverse slices were used to create a computerized 3-dimensional volume array modeling all major internal structures of the body. The original x-ray CT images were reconstructed in a 512x512 matrix with a resolution of 1 mm in the x,y plane. The z-axis resolution is 1 cm from neck to mid-thigh and 0.5 cm from neck to crown of the head. The final phantom is interpolated to create a 128x128x243 byte volume giving a 4x4x4 cubical mm voxel size dimension [13]. Each voxel of the volume contains an index number designating it as belonging to a given organ or internal structure.

IV. RESULTS

In order to validate the proposed parallel FDTD code, we present now in Fig. 1 some numerical results for a real RBA, the Kathrein (K) 730685, whose dimensions are reported in the same Fig. 1. The simulated radiation patterns (RP) both in the E and H-plane are evaluated using an observation distance of almost 6 m, and compared with the vendor's data. Also, a color representation of the levels of the electric field in both the vertical and horizontal planes is reported in the same Fig. 1. It can be observed that a very good accuracy is achieved.

As further validation, a conspicuous number of simulations on the most common canonical cases has been performed. For instance, a 3-layered sphere (skin+bone+brain) has been exposed to the EM-field of a 900 MHz half-wave dipole. The radiated power is 1W, the external sphere radius is 10 cm, the feeding gap is 2.5 mm and the distance between the feed and the sphere surface is almost 6 mm. The local SAR, the SAR averaged over 1g of tissue (1g-SAR) and over 10g of tissue (10g-SAR) have been evaluated and the power absorbed by the head has been estimated. The implemented simulation scheme and the adopted reference system are shown in Fig 2. In the same Fig. 2, the behaviour of the 10g-SAR is reported. The result of Fig. 2 is in a very good agreement with data reported in [17].

Among the possible applications, the developed parallel FDTD tool can be used to verify the accuracy of several experimental set-ups, using a homogeneous phantom approximation. The human exposure to the near field of a RBA has been solved using two different numerical phantoms: the VHP heterogeneous phantom described in Section III, and a homogeneous phantom with the same shape of the VHP one, though modeled with constant dielectric characteristics in each point (ε_r=43 and σ=0.83 S/m). The phantoms have been exposed to a real antenna (K730678), varying the mutual position and the distance between antenna and phantom; the maximum studied distance is 60 cm. The following parameters are estimated:

a) the local SAR, the 1g-SAR and the 10g-SAR, in each point of the studied phantoms;
b) the peak SAR both for 1g-SAR and 10g-SAR, in the phantom head and in the phantom trunk;
c) the power absorbed by the phantoms (full-body, head, brain, trunk and heart).

The domain is partitioned into 320x320x256 cubic cells, the radiated power is 32 W and the operating frequency is 902 MHz.

The obtained results can be summarized as follows:

- both the position and the value of the maximum evaluated SAR are similar in the studied phantoms, for each RBA-phantom distance and mutual position;
- the values of the SAR averaged over a large portion of human body, like the head or a portion of it, the bust or the trunk, are comparable in both cases;
- the comparison of the punctual values of the dosimetric parameters, instead, put forwards substantial differences between the use of a heterogeneous phantom rather than a homogeneous one. In fact, because of the different position of the local maxima and minima, a 40% difference, in some investigated phantom's points, can be observed.

Fig 3. The qualitative E-field levels for one of the several implemented exposure conditions. The use of the VHP phantom (left) rather than the homogeneous one (right), causes substantial differences in the estimated SAR levels.

We recall now that the ICNIRP guideline recommends 3 different safety limits for workers:

1) whole body average SAR : 0.4 W/Kg;
2) 10-g SAR in each head or trunk point: 10 W/Kg;
3) 10-g SAR in each limbs point: 20 W/Kg.

In all the simulated cases the whole-body average SAR is substantially smaller than the reference value. On the contrary, a more careful analysis and discussion must be performed (and is here omitted for the sake of conciseness) for the remaining two limits, which are in some cases exceeded.

In Fig. 3, the qualitative representation of the E-field levels is shown in a vertical section of one of the simulated cases (the human-antenna distance is 30cm). The antenna and the phantom's shape are easily identifiable and the colour scale from blue to red put forwards the different field levels, both for VHP and for the homogeneous phantom (red colour is for high E-field intensity). For this simulation, as an example, the estimated peak 1g-SAR is 13.12 W/Kg for the VHP phantom, against 12.42 W/Kg for the homogeneous one (see Fig. 4); the SAR averaged over a large portion of the head is comparable too (0.39 W/Kg against 0.35 W/Kg), but a maximum absolute difference of almost 4 W/Kg has been calculated in the 1g-SAR estimation.

V. Conclusion

In this paper a parallel FDTD tool is presented, suitable for the solution of large dosimetric problems. The tool is first validated on experimental and numerical data, and then used to solve a relevant problem, such as the human exposure to the near-field of radiobase antennas.

Fig 4. The 1g-SAR levels in the phantom head for the exposure condition reported in Fig. 3. A zone with high SAR differences is marked.

The attained results demonstrate the accuracy of the approach, as well as its amenability to solve very large problems. A specific discussion is also performed on the use of homogeneous simplified human phantoms with respect to accurate heterogeneous phantoms.

VI. Acnowledgment

Many thanks to CNR – Agenzia 2000 for the financial support to the current project

References

[1] A. D. Tinniswood, C. M. Furse, O. P. Gandhi, "Computations of SAR distributions for two anatomically based models of the human head using CAD files of commercial telephones and the parallelized FDTD code", *IEEE Trans. on Ant. Prop.*, 46, 6, pp. 829-833, 1998.

[2] K. Nikita et al., "A Study of Uncertainties in Modelling Antenna Performance and Power Absorption in the Head of a Cellular Phone User", *IEEE Trans. on MTT*, vol 48, 12, pp. 2676-2686, 2000.

[3] P. Bernardi, M. Cavagnaro, S. Pisa, E. Piuzzi, "Human Exposure to radiobase station antennas in urban environment", *IEEE Trans. on MTT*, vol 48, 11, pp. 1996-2003, 2000.

[4] A. Bahr, D. Manteuffel, D. Heberling: "Occupational safety in the near field of a GSM base station", *Proc. of AP2000*, Davos, April 2000, 3A6.7.

[5] K. Ito, L. Hamada, T. Asahina, H. Yoshimura, "Phantoms for Estimation of Interaction between Antenna and Human Body", *Proc. of AP2000*, Davos, April 2000, 3A6.8.

[6] J. D. Kraus: 'Antennas'. Mc Graw Hill – 1988.

[7] G. Mur, "Absorbing boundary conditions for the Finite-Difference approximation of the Time-Domain Electromagnetic-Field equations", *IEEE Trans. on EM Comp.*, vol. EMC-23, 4, pp. 377-382, 1981.

[8] J.-P. Berenger, "A perfectly matched layer for the absorption of electromagnetic waves", *J. Computational Physics*, vol. 114, 1994.

[9] J.-P. Berenger, "A perfectly matched layer for the FDTD solution of wave-structure interaction problems", *IEEE Antennas Propag. Symp.*, vol. 44, n.1, 1996.

[10] A. Taflove and M. E. Brodwin, "Numerical solution of steady-state electromagnetic scattering problems using the time-dependent Maxwell's equations", *IEEE Trans. on MTT*, vol. 23, 8, pp. 623-630, 1975.

[11] A. Taflove, 'Computational Electrodynamics: The Finite-Difference Time-Domain Method', Norwood, MA, Artech House, 1995

[12] C. Battista et al., "The APE100 Computer: (I) the Architecture", *Int. Journal of High Speed Computing* n. 5 1993.

[13] I. G. Zubal, C. R. Harrell, E. O. Smith, Z. Rattner, G. Gindi, P. B. Hoffer, "Computerized 3-Dimensional Segmented Human Anatomy", *Medical Physics, 21(2), pp* 299-302, February 1994.

[14] C. Gabriel, S. Gabriel, E. Corthout, 'The dielectric properties of biological tissues: I Literature Survey', *Phys. Med. Biol.*, vol. 41, pp.2231-2249, 1996.

[15] C. Gabriel, 'Compilation of the Dielectric Properties of Body Tissues at RF and Microwave Frequancies', *Brooks Air Force Technical Report AL/OE-TR*-1996-0037.

[16] P. A. Mason et al., 'Effects of Frequency, Permittivity and Voxel Size on Predicted SAR values in biological tissues during EMF Exposure', *IEEE Trans. on MTT*, vol 48, 11, pp. 2050-2061, 2000.

[17] K. Nikita, G. Stamatakos, N. Uzunoglu, A. Karafotias, 'Analysis of the InteractionBetween a Layered Spherical Human Model and a Finite-Lenght Dipole', *IEEE Trans. on MTT*, vol 48, 11, pp 2003-2012, 2000.